

Investigation of the Bed and Structural Slopes on Bed Shear Stress and Flow Characteristics around an Impermeable Groyne

1. R. Ghaldarbandi

Department of Civil Engineering, Sahand
University of Technology, Tabriz, I.R. of IRAN

2. M.H. Keshavarz

Department of Civil Engineering, Sahand University of
Technology, Tabriz, I.R. of IRAN

3. H. Hakimzadeh

Department of Civil Engineering, Sahand University of
Technology, Tabriz, I.R. of IRAN, hakimzadeh@sut.ac.ir

Abstract

In this paper, effects of the cross shore and groyne wall slopes on flow parameters around an impermeable groyne were considered using a three-dimensional numerical CFD model (i.e., FLUENT). The $k-\epsilon$ turbulence model was used to evaluate the Reynolds stresses. The model was first applied to a vertical groyne on a flat bed and the model results were compared with the relevant experimental data. The results of this numerical test showed good agreements with the corresponding experimental measurements, in terms of water elevation, velocity magnitudes and reattachment length. The model was then applied to a series of structures with different lateral wall slopes on various cross sectional bed slopes. The numerical model results revealed that by increasing the cross shore bed slope in any case of the structural slopes, the magnitude of the maximum velocity and bed shear stresses decreased. These values decreased further as the structural slope reduced.

Keywords: *Flow characteristics, Bed shear stress, Impermeable groyne, Bed and structural slopes, Turbulence model, Numerical simulati*

1 Introduction

The groynes which are typical of shore protective structures can provide several aims. Although these structures may partly help to shoreline protection, however, they would create some major problems such as scour phenomenon in the adjacent regions. In the past, due to poor considerations of the problems related to river structures including: design principles, technical properties and the methods of deploying these structures such as groynes which are frequently used to shore protection of the rivers, a number of them partly and/or completely failed. Also some of these structures were unsuccessful against river reactions and even intensely caused undesirable conditions. Installing groynes is one of the most effective approaches to stabilize eroding river banks and to sustain navigable channels at a proper depth and location by directing flow away from the banks and toward the main channel. The presence of these structures have been shown to have environmental benefit as they increase aquatic habitat (Shields et al. [1]) by providing large stable pools and complex channel bathymetry (scour holes) for fish and to enhance the bio-diversity of flora and fauna in rivers. Also, in order to investigate the scouring process and ultimately estimating the scour depth, it is necessary to describe the coherent structures present in the flow and to quantify their effect on river bed

near the groyne base including any increasing in local bed shear stress and turbulence fluctuations, as these two parameters can be considered the key factors for the sediment transport and consequently erosion phenomenon (Fredsoe and Deigaard [2]). On the other hand, one of the major interests in numerically simulating such flows is to reproduce properly the recirculating flow downstream of the groyne to make a progress in designing the dikes. Also, it is generally admitted that the non-dimensional reattachment length (the separated length of flow to the groyne length) is influenced mainly by the eddy viscosity field and most of the authors dealing with dike designing focus on the corrections to be brought to the standard turbulence models in order to improve them for recirculating flows (Ouillon and Dartus [3]). In addition, the effects of groyne layout on the flow in groyne fields have experimentally been studied by Uijtewaal [4]. These experiments were conducted on a same bed cross-shore slope (i.e. 1:30) and for a few structural slopes. In the current study, however, a wide range of bed cross-sectional and structural slopes will be considered numerically. For the past few years, a number of researches dealing with the flow structures and scour process around the groynes have been carried out both experimentally and numerically including: Molls et al. [5], Tominaga et al. [6], Zhou et al. [7], Uijtewaal et al. [8],

Kuhnle et al. [9], Ettema et al. [10], Yossef [11], Nagata et al. [12] and more recently, Xuelin et al. [13].

2 Model Verification

The Fluent software which is a computational fluid dynamic (CFD) tool has been used for the current research. The time-averaged Reynolds equations of motion for a three-dimensional flow are now widely used by the researchers and with the CFD software but not given here for brevity. Also, there are varieties of turbulence models for the Reynolds stresses calculations in the model. For the current study, various turbulence models have been used to calculate the Reynolds stresses and it was found that the numerical model results of the k-e RNG turbulence model were in very good agreement with the experimental measurements. For this model, there is an extra term in the epsilon equation when compared with the standard k-e equations. The extra term increase its accuracy for the rotational flows. Also, the constant Prandtl numbers in the k-e equations are determined using analytical relationships and the model is thus appropriate for the low Reynolds number flows. In addition, the model has mostly been used for the flow fields of complex geometries and reasonable numerical model results have been achieved. More details of the k-e RNG turbulence model can be found in the literatures (see Chen and Jaw, [14]) and software user's guide and again are not given here for brevity. For the numerical model reported herein, the finite volume method has been used to discretize the governing equations. The finite volume method used in the software makes attractive flexibility to use any shape of grids to cover the bed cross-shore and structural slopes in computational domain. Also, an explicit method has been used for solving the resultant equations. In order to verify the numerical model predictions for the current research field, the model was firstly run for the similar model data of Ouillon and Dartus [3]. Therefore, the numerical setup was based on the physical model of Holtz [15] (cited in Ouillon and Dartus [3]) which was a channel with 30m long, 2.5m width and smooth vertical walls. A rectangular groyne with a dimension of 25cm in length and 2.5cm in width was set in the middle of model channel on a side (Figure. 1).

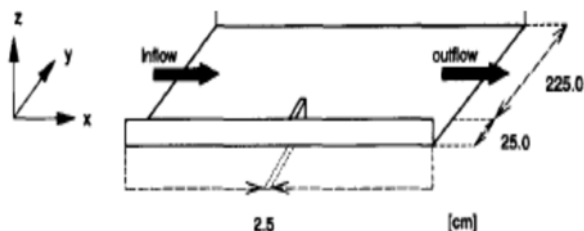


Fig.1 Flow configuration around the groyne (Holtz, [15])

The numerical model was run for turbulent flow conditions of the mean water depth of 0.23m and the mean flow velocity in the undisturbed zone of 0.345m/s. Also, the air phase thickness was set to be 0.1m. Thus, for the upstream open boundary and water phase, a velocity inlet was set to be 0.345m/s. likewise, in order to maintain the water depth in the main channel, a suppressed weir with 12cm height was set at the downstream open boundary condition. For these open boundaries, the length scale and turbulent intensity were determined according to the formulae given in user's guide of the Fluent [16]. In addition, different types of surface boundary including the rigid lid and volume of fluid (VOF) have been tested in the numerical model and it was found that the VOF condition was the most appropriate one for the water surface (see Keshavarz et al. [17]). Then, this method has been deployed for all consequent numerical tests. For the air phase, the inlet and outlet pressure conditions were used at the open upstream and downstream boundaries of the channel. The local relative pressure was set to be zero and relatively small values of the turbulent parameters were selected for these boundaries. The common no-slip boundary condition was used for the solid boundaries. The numbers of layers for the water and air phases were 6 and 2, respectively. The thicknesses of the layers varied with depth, with the small and large values were set nearby the channel bed and free surface, respectively.

The comparisons have then been made between the numerical model results and corresponding experimental measurements of the water elevation and velocities magnitudes and reattachment length. Figure 2 shows the reproduced graphical model results for the water elevation around the groyne together with the experimental data and model results of Ouillon and Dartus [3].

It is evidence of this object that the method of VOF has appropriate ability in prediction of water surface elevations. It can also be seen from the figure that the agreements between the model results and laboratory measurements are fairly good and the model results of the current study are similar to the model results of Ouillon and Dartus. furthermore, the predicted model results for the velocity fields around the groyne on the planes at $z=+0.17\text{m}$ and $z=+0.05\text{m}$ above bed are shown in figures 3 and 4, respectively. The corresponding model results of Ouillon and Dartus together with experimental measurements are also shown here.

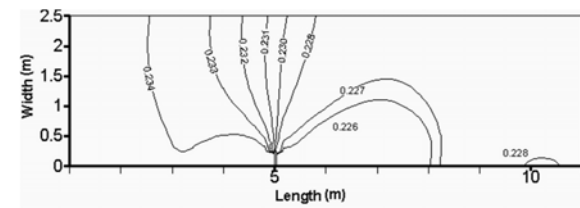
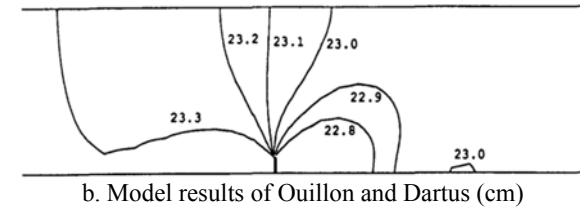
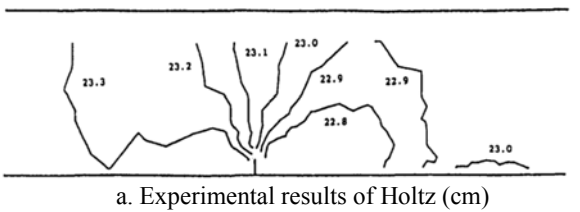


Fig.2 Isolines of water elevations around the groyne

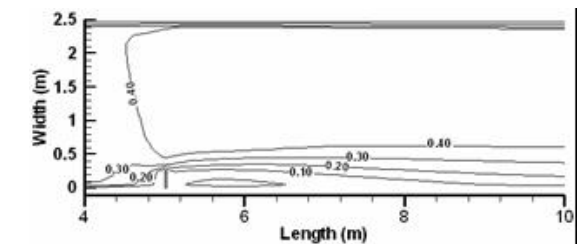
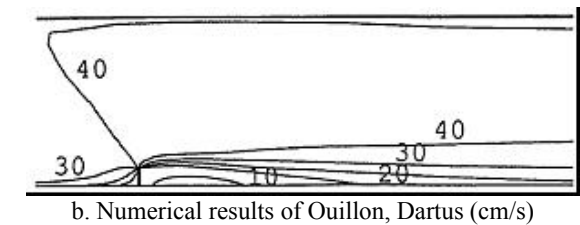
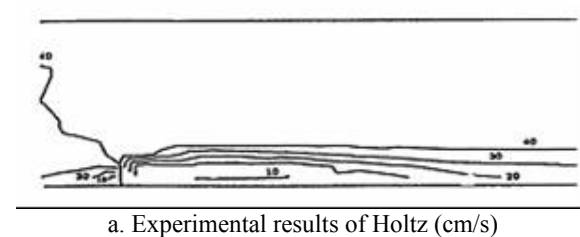


Fig.3 Isolines of velocity around the groyne at $z=+0.17m$

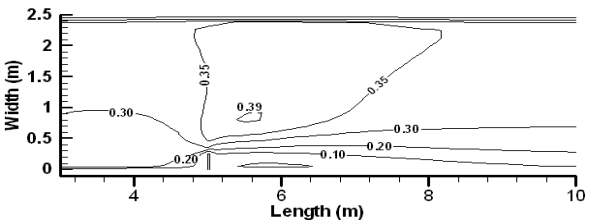
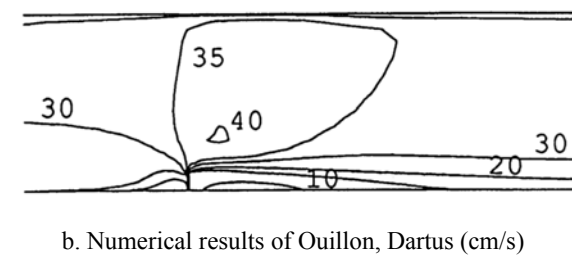
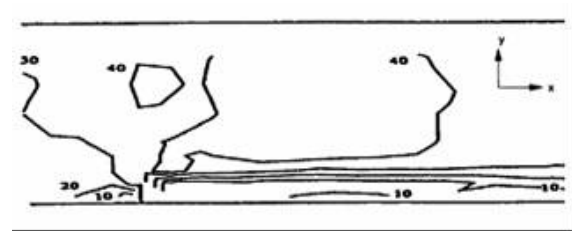


Fig.4 Isolines of velocity around the groyne at $z=+0.05m$

Again, as can be seen from the figures, the reproduced model results of the current study are in good agreement with the observation data in the laboratory and similar to those of Ouillon and Dartus. Moreover, the predicted numerical model non-dimensional reattachment length at $z=+0.17m$ was 11.2 from the research study whereas the length were 11.5 based on experimental data of Holtz[15] and 10.7 based on the numerical model results of Ouillon and Dartus [3]. This issue will further be discussed in the next sections.

3 Model Configurations

The main aim of the current study was to examine the effects of the cross-sectional bed slope of the river and structural slope of the groyne on the flow pattern, maximum magnitude of velocity and non-dimensional reattachment length. The model was thus run for the various slopes of cross-sectional bed (i.e. 0%, 5% and 10%) and groyne-wall (i.e. 1:0, 1:1, 1:2, 1:3). Some of the typical geometry shapes

of groynes on various cross-sectional bed slopes are shown in figures 5 and 6.

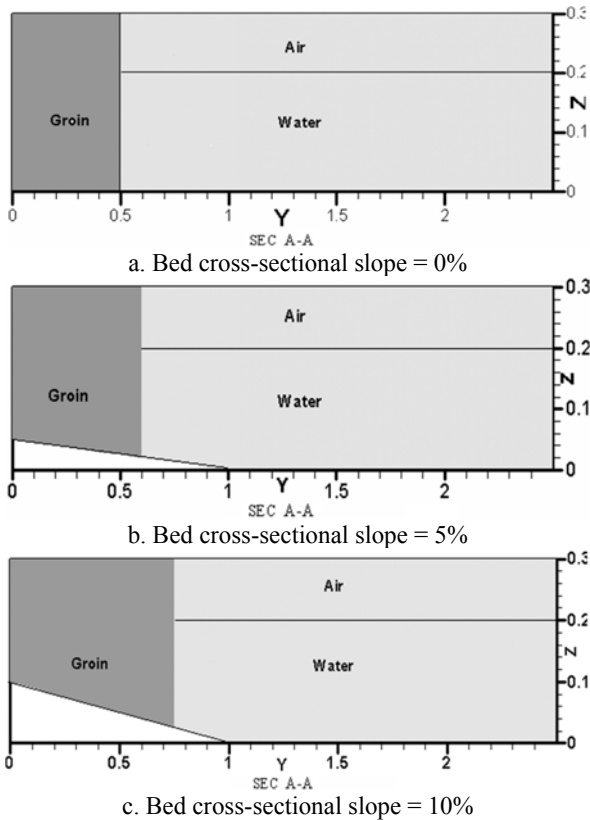


Fig.5 Geometry shapes of cross-sectional for the vertical groyne

4 Model Applications

The numerical simulation was then performed on a channel with 20m long, 2.5m wide and 0.3m height containing 0.2m water phase and 0.1m air phase. Numbers of layers for the water and air phases were 6 and 2 respectively. The groyne was set in the middle channel length and perpendicular to a side of the channel. For all model simulation the cross-sectional area that is blocked by the groyne was kept constant and set to be 0.1m². Therefore by increasing the cross-sectional bed slope, the groyne length increased since the blocked area was kept constant. For the upstream open boundary (i.e. the undisturbed zone) and water phase, a inlet velocity was set to be 0.345m/s. Also, in order to maintain the water depth in the main channel, a suppressed weir with 10cm height was set at the downstream open boundary condition. The other conditions were similar to those used for the verified model. Then, the grid systems of the plan views are shown in Fig. 7. For the sloped sidewall model configurations a complex mesh containing of the tetrahedron and hexahedron meshes was used. A typical grid system on vertical plane is also shown in Fig. 8. The number of layers

in vertical direction was equal for all model configurations and was set to be 8.

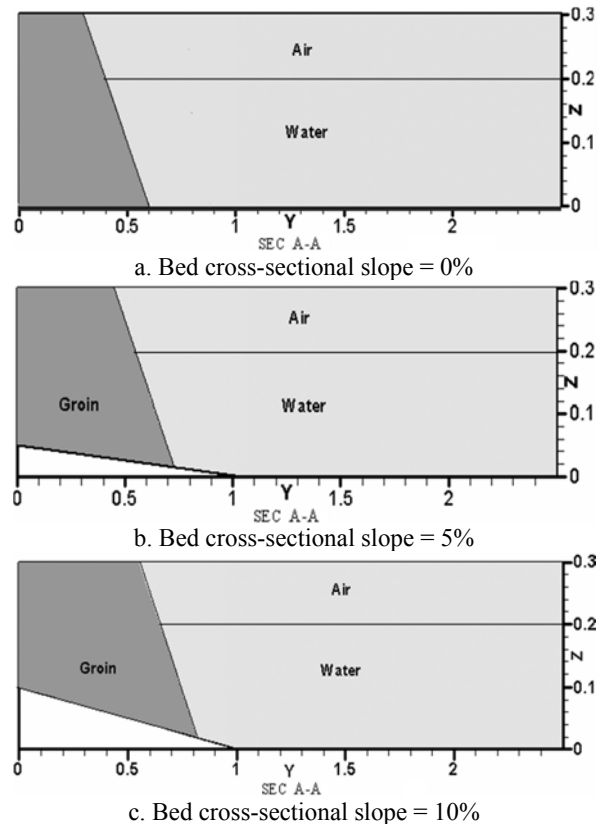


Fig.6 Geometry shapes of cross-sectional for the groyne with sidewall slope = 1:1

5 Model Results: Velocity Fields

For this section, the numerical model results for the magnitudes of velocities at four levels of water column are presented. Then the model results for the bed shear stress, reattachment length and water elevation are presented in the next sections.

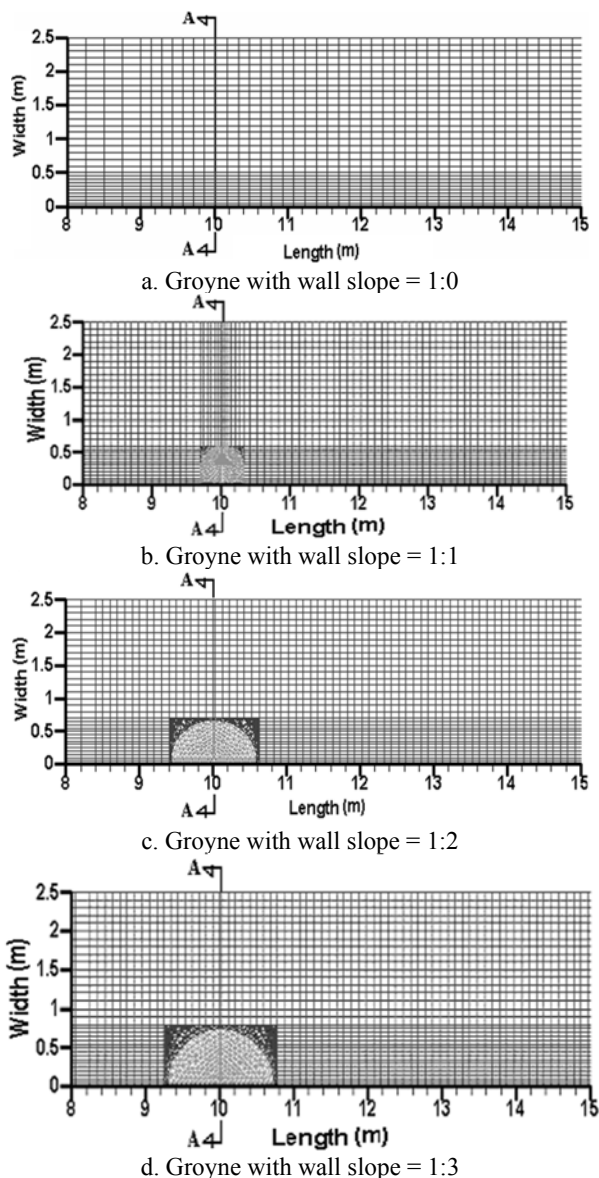


Fig.7 Plan views of grid systems around the groyne on a flat bed

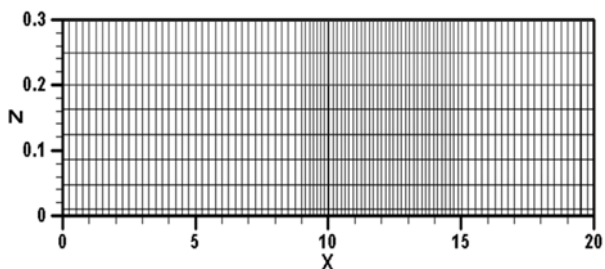


Fig.8 Grid system around vertical groyne on flat bed in the vertical plane

5.1) Velocity fields

Firstly, the numerical model results showed that the magnitudes of the velocities were gradually increased with depth and the maximum values were occurred at a level nearby to the free surface (i.e. the top layer). This was predictable since the shear stresses reduced at this water level. secondly It has been found that by increasing of the cross-sectional bed slope the maximum velocity magnitude and its domain decreased. For this case and similar to the compound channels, due to conduction of main flow to the main channel the unit flow decreased at the side of channel, where the groyne was set. Also the model results have shown that by decreasing the slope of groyne-walls (i.e. structural slope) the velocities magnitudes decreased correspondingly as the turbulent intensity created in the vicinity of the groyne was gradually decreased. The maximum magnitudes of velocities for the various cross-sectional bed and structural slopes at different levels of water depth are shown in table 1. It can obviously be seen from the table that by increasing the bed slope, the maximum values of the velocities decreased at different water levels. For example, for the groyne-wall slope of 1:0, the predicted maximum velocity at water surface on a flat bed is 0.68m/s, whereas the corresponding value for the 10 percent cross-sectional bed slope is 0.61m/s. Comparing of these values indicates that the maximum value decreased about 10 percent. Similarly, comparing the corresponding bed layer results indicates that the maximum value decreased about 34 percent. Also the numerical model results have shown that by decreasing the structural slope of the groyne the corresponding values further decreased. This can be found by comparing the corresponding maximum values of the different structural slopes. Here, another example can be shown for the maximum values of the bed layers. For instance, for the groyne-wall slope of 1:0 (i.e. vertical wall), the predicted maximum velocity adjacent to the water surface on a flat bed is 0.68m/s, whereas the corresponding value for the groyne-wall slope of 1:3 is 0.56m/s. Again, comparing of these values indicates that the maximum value decreased about 18 percent. Similarly, comparing the corresponding bed layer results indicates that the maximum value decreased about 26 percent. Then, it can be concluded from the numerical model results that the rate of decreasing for the bed layers are greater than that for the top layers. Similar results can be achieved by comparing the velocity fields for different bed slopes.

Table 1 Maxima values of the velocities

Model of Groyne	Wall Slope	Bed Cross-Slope (%)	Level (m)	Maximum Value of Velocity (m/s)
1	1:0	0	0.015	0.38
1	1:0	0	0.05	0.54
1	1:0	0	0.1	0.62
1	1:0	0	0.2	0.68
2	1:0	5	0.015	0.29
2	1:0	5	0.05	0.54
2	1:0	5	0.1	0.60
2	1:0	5	0.2	0.64
3	1:0	10	0.015	0.25
3	1:0	10	0.05	0.48
3	1:0	10	0.1	0.56
3	1:0	10	0.2	0.61
4	1:1	0	0.015	0.30
4	1:1	0	0.05	0.51
4	1:1	0	0.1	0.58
4	1:1	0	0.17	0.62
5	1:1	5	0.015	0.27
5	1:1	5	0.05	0.49
5	1:1	5	0.1	0.57
5	1:1	5	0.2	0.58
6	1:1	10	0.015	0.25
6	1:1	10	0.05	0.44
6	1:1	10	0.1	0.51
6	1:1	10	0.2	0.56
7	1:2	0	0.015	0.29
7	1:2	0	0.05	0.51
7	1:2	0	0.1	0.58
7	1:2	0	0.2	0.60
8	1:2	5	0.015	0.26
8	1:2	5	0.05	0.48
8	1:2	5	0.1	0.54
8	1:2	5	0.2	0.55
9	1:2	10	0.015	0.25
9	1:2	10	0.05	0.40
9	1:2	10	0.1	0.48
9	1:2	10	0.17	0.54
10	1:3	0	0.015	0.28
10	1:3	0	0.05	0.48
10	1:3	0	0.1	0.53
10	1:3	0	0.2	0.56
11	1:3	5	0.015	0.27
11	1:3	5	0.05	0.46
11	1:3	5	0.1	0.51
11	1:3	5	0.2	0.54
12	1:3	10	0.015	0.25
12	1:3	10	0.05	0.40
12	1:3	10	0.1	0.47
12	1:3	10	0.2	0.50

Fig. 9 illustrates a graphical comparison of the velocity fields for the vertical groyne-wall with different cross-sectional bed slopes at the water surface.

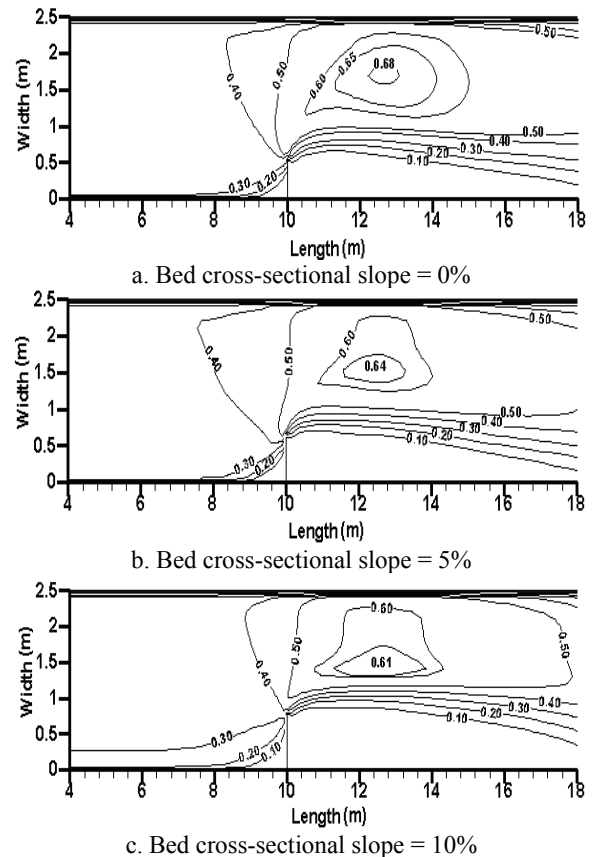


Fig.9 Isolines of velocities at $z=+0.2m$ for the vertical groyne

Similarly, Fig. 10 illustrates the predicted velocity fields for different structural slopes of the groyne on a flat bed. Again, it can be seen that by decreasing the structural slope of the groyne, the maximum velocity decreased consequently.

5.2) Bed shear stress

The numerical model results for the bed shear stress and for different model configurations on various cross-sectional bed slopes are presented in this section. The maximum magnitudes of bed shear stresses for the various cross-sectional bed and structural slopes are shown in table 2.

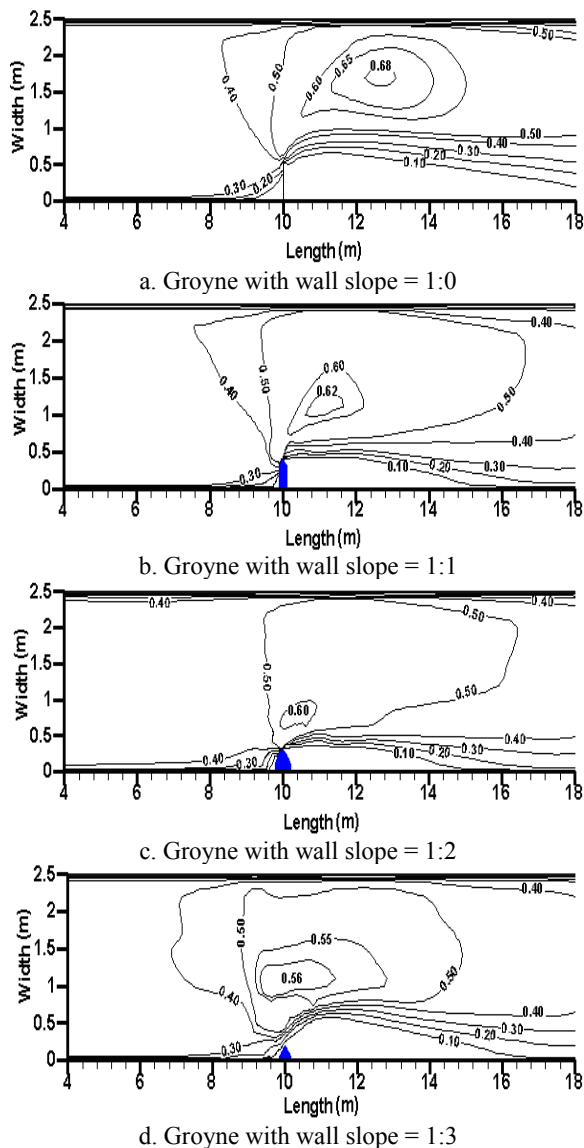


Fig.10 Isolines of velocities at $z=+0.2m$ for the flat bed

Table 2 Maximum values of bed shear stresses

Model of Groyne	Wall Slope	Bed Cross-Slope (%)	Maximum Value of the Bed Shear Stress (pa)
1	1:0	0	1.8
2	1:0	5	1.6
3	1:0	10	1.2
4	1:1	0	1.4
5	1:1	5	1.2
6	1:1	10	0.9
7	1:2	0	1.3
8	1:2	5	1.2
9	1:2	10	0.8
10	1:3	0	1.2
11	1:3	5	1.1
12	1:3	10	0.8

It can clearly be seen from the table that by increasing the bed slope, the maximum values of the bed shear stresses reduced consequently. For example, for the groyne-wall slope of 1:0, the predicted maximum bed shear stress on a flat bed is 1.8pa, whereas the corresponding value for the 10 percent cross-sectional bed slope is 1.2pa. Comparing of these values indicates that the maximum value decreased about 33 percent.

Also the model results have shown that by decreasing the structural slope of the groyne the corresponding values for the bed shear stresses further decreased. This can be found by comparing the corresponding maximum values of the different structural slopes. For instance, for the groyne-wall slope of 1:0, the predicted maximum bed shear stress on a flat bed is 1.8pa, whereas the corresponding value for the groyne-wall slope of 1:3 is 1.2pa. Again, comparing of these values indicates that the maximum value decreased about 33 percent. In comparing all of the model results, it can be concluded that by increasing the cross-sectional bed slope and decreasing the structural slope of the groyne, the magnitudes of bed shear stresses reduced.

Similar results can be achieved by comparing the bed shear stress fields for different bed slopes. Fig. 11 illustrates a graphical comparison of the bed shear stress fields for the vertical groyne-wall and for different cross-sectional bed slopes. Here, it can be seen that in any case the maxima of the bed shear stresses were produced at the tip of the groyne. Thus, since the bed shear stress can be regarded as a key factor of scour process, it can be predictable that the threshold of scour process will be occurred at the head of the groyne.

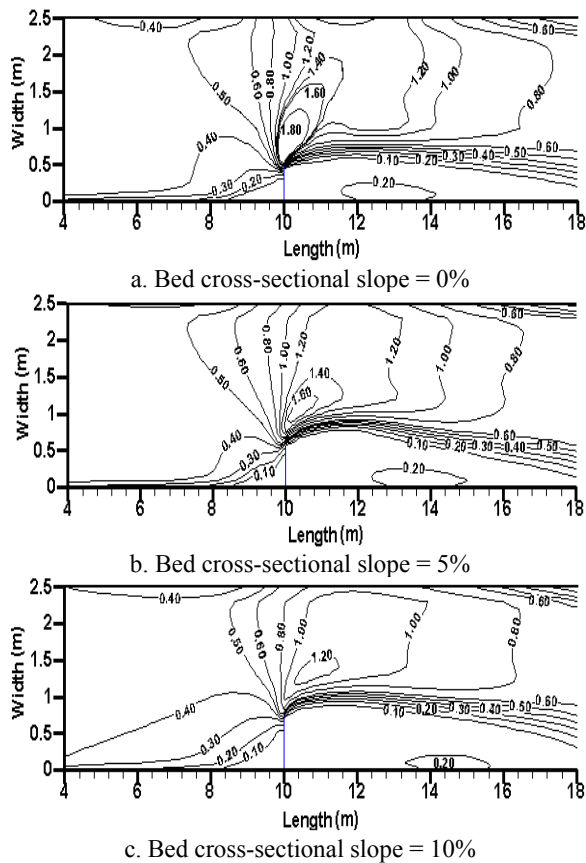


Fig.11 Isolines of bed shear stresses for the vertical groyne

Similarly, Fig. 12 illustrates the predicted bed shear stress fields for different structural slopes of the groyne on the flat bed. Again, it can be seen that by decreasing the structural slope of the groyne, the maximum value of the bed shear stress decreased. Then, it can be concluded that by decreasing the bed shear stress the scour process may be reduced in adjacent the structures.

5.3) Reattachment length

The numerical model results of the streamlines are presented in this section. Reattachment point is the location where the separated flow reattaches the channel wall downstream of the groyne. Fig. 13 illustrates the streamlines adjacent to the groyne for the vertical groyne-wall with different cross-sectional bed slopes at a level near the water surface. The model results have shown that by increasing the cross-sectional bed slope, the reattachment length increased. However, the non-dimensional length of the reattachment (reattachment length/groyne length) was reduced since the length of groyne increased correspondingly. Moreover, secondary circulation cells grew adjacent to the groyne when the cross-sectional bed slope increased. The main circulation cell in the downstream part of the groyne rotated in

clockwise direction while the secondary gyre rotated in counterclockwise direction.

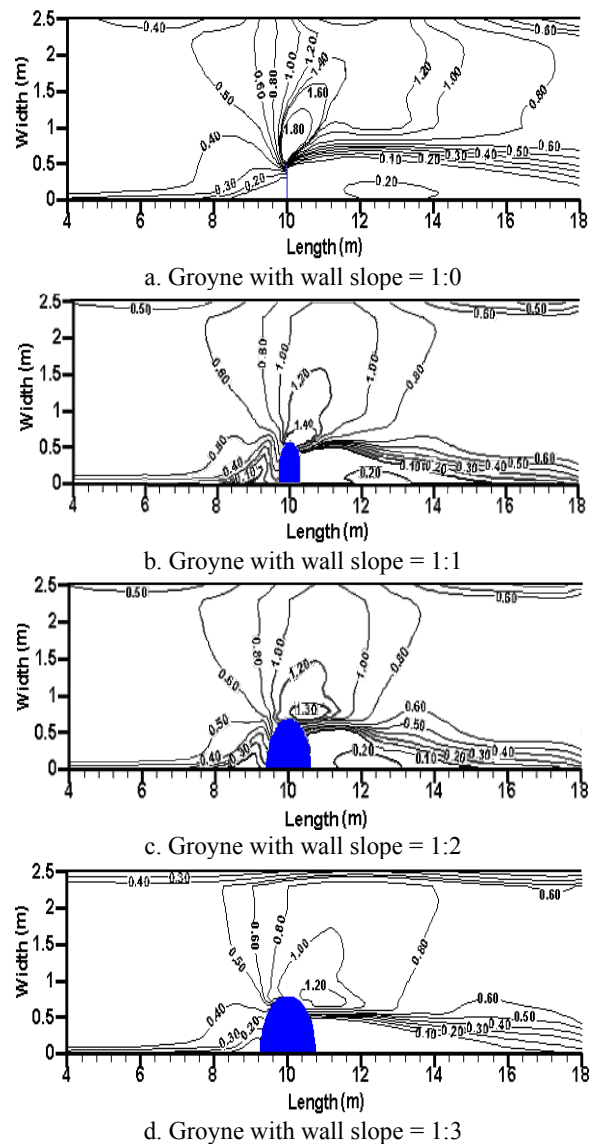


Fig.12 Isolines of bed shear stresses for the flat bed

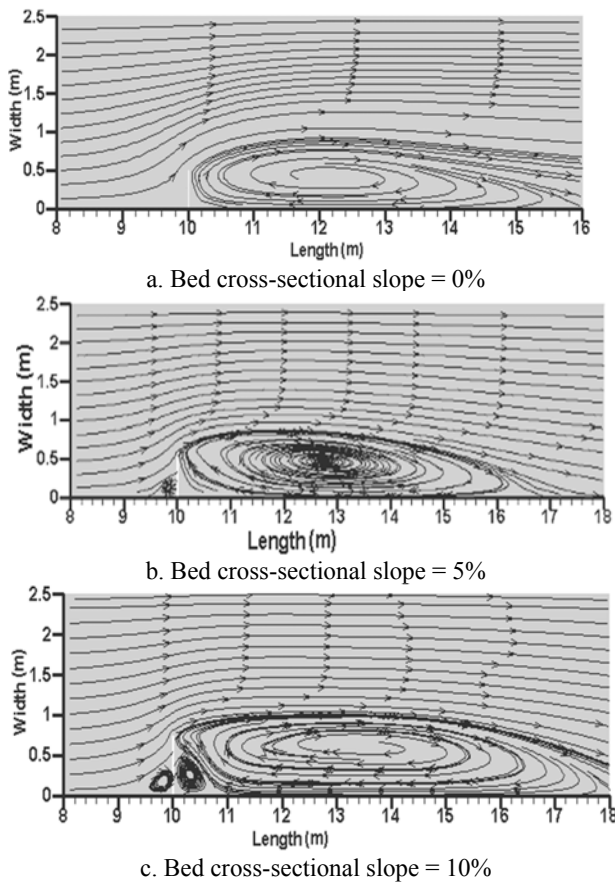


Fig.13 Streamlines at $z=0.175\text{m}$ around the vertical groyne

The other numerical tests have shown that by decreasing the structural slope of the groyne, the reattachment length decreased and the maximum reattachment length occurred around the vertical groyne (see Fig. 14).

Also, the down and swirling flows produced at the upstream and downstream of groyne in the vertical plane. The structures of these flows will further be discussed in the next section. The magnitudes of reattachment lengths for the various cross-sectional bed and structural slopes are also shown in table 3.

5.4) Velocity vectors fields in the vertical plane

In this section, details of predicted vertical swirling flows at the upstream and downstream groyne are presented. These down-flows can be regarded another key factor of the groynes' scour at their sidewalls. The typical numerical model results of the vertical swirling flows for the vertical and relatively sloped groynes at a distance from channel wall (i.e. $y=0.25\text{m}$) and for different cross-sectional bed slopes are shown in Figs. 15 and 16, respectively.

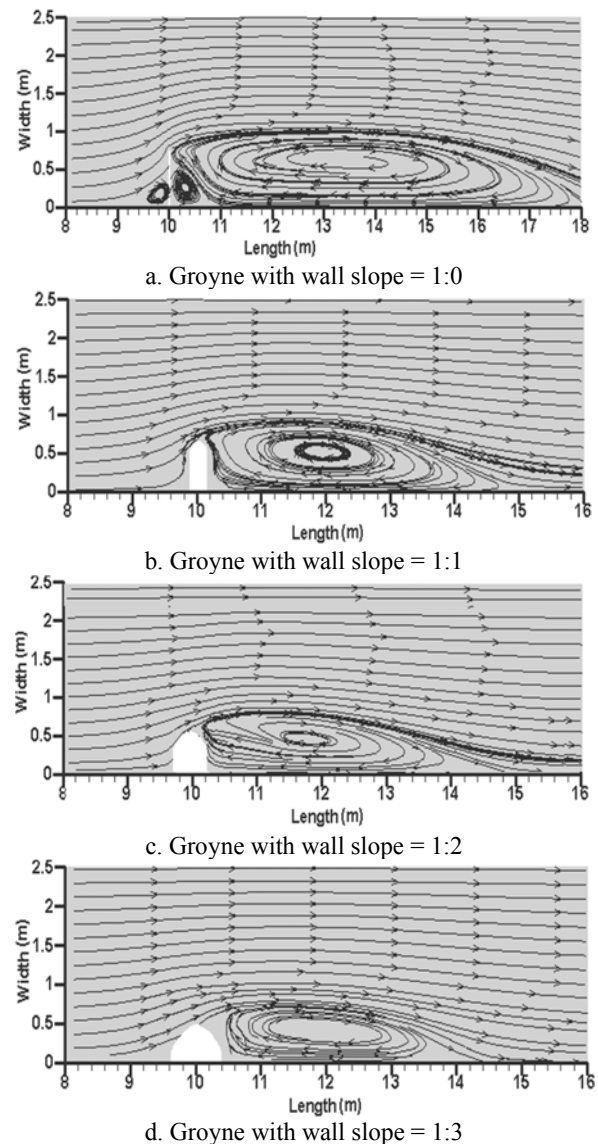
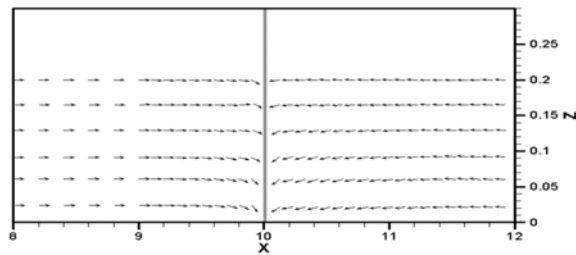


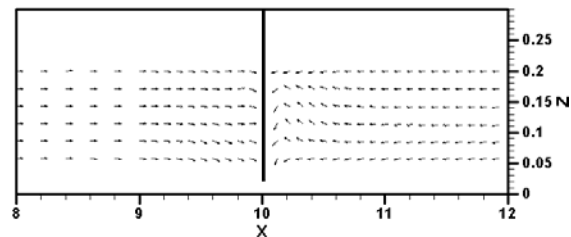
Fig.14 Streamlines at $z=0.175\text{m}$ for the bed cross-sectional slope = 10%

Table 3 Reattachment length at the various water levels for the various bed and structural slopes

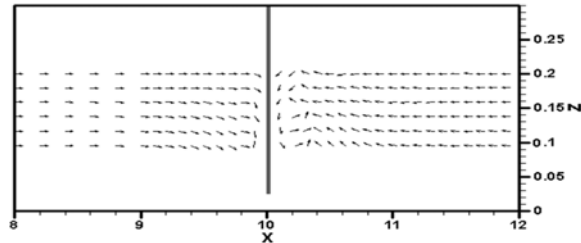
Model of	Wall	Bed Cross-	Level	Length of	Reattachment Length	Non-Dimensional
1	1:0	0	0.015	0.5	5.2	10.4
1	1:0	0	0.05	0.5	5.3	10.6
1	1:0	0	0.1	0.5	4.8	9.6
1	1:0	0	0.175	0.5	5.4	10.8
2	1:0	5	0.015	0.0	-	-
2	1:0	5	0.05	0.6	6.0	10.0
2	1:0	5	0.1	0.6	6.2	10.3
2	1:0	5	0.175	0.6	6.3	10.5
3	1:0	10	0.015	0.0	-	-
3	1:0	10	0.05	0.25	-	-
3	1:0	10	0.1	0.75	7.5	10.0
3	1:0	10	0.175	0.75	7.75	10.3
4	1:1	0	0.015	0.585	4.6	7.9
4	1:1	0	0.05	0.55	4.5	8.2
4	1:1	0	0.1	0.5	4.0	8.0
4	1:1	0	0.175	0.425	4.0	9.4
5	1:1	5	0.015	0.03	-	-
5	1:1	5	0.05	0.70	5.1	7.3
5	1:1	5	0.1	0.65	4.9	7.5
5	1:1	5	0.175	0.575	4.6	8.0
6	1:1	10	0.015	0.0	-	-
6	1:1	10	0.05	0.32	-	-
6	1:1	10	0.1	0.75	5.0	6.7
6	1:1	10	0.175	0.675	4.7	7.0
7	1:2	0	0.015	0.67	4.7	7.0
7	1:2	0	0.05	0.60	4.5	7.5
7	1:2	0	0.1	0.50	3.9	7.8
7	1:2	0	0.175	0.35	3.2	9.1
8	1:2	5	0.015	0.10	-	-
8	1:2	5	0.05	0.75	5.0	6.7
8	1:2	5	0.1	0.65	4.7	7.2
8	1:2	5	0.175	0.50	4.0	8.0
9	1:2	10	0.015	0.06	-	-
9	1:2	10	0.05	0.41	-	-
9	1:2	10	0.1	0.75	4.6	6.1
9	1:2	10	0.175	0.60	4.0	6.7
10	1:3	0	0.015	0.755	4.3	5.7
10	1:3	0	0.05	0.65	4.1	6.3
10	1:3	0	0.1	0.50	3.5	7.0
10	1:3	0	0.175	0.275	2.5	9.1
11	1:3	5	0.015	0.20	-	-
11	1:3	5	0.05	0.85	4.6	5.4
11	1:3	5	0.1	0.70	4.2	6.0
11	1:3	5	0.175	0.475	3.4	7.2
12	1:3	10	0.015	0.20	-	-
12	1:3	10	0.05	0.55	-	-
12	1:3	10	0.1	0.75	4	5.3
12	1:3	10	0.175	0.525	3.3	6.3



a. Bed cross-sectional slope = 0%



b. Bed cross-sectional slope = 5%

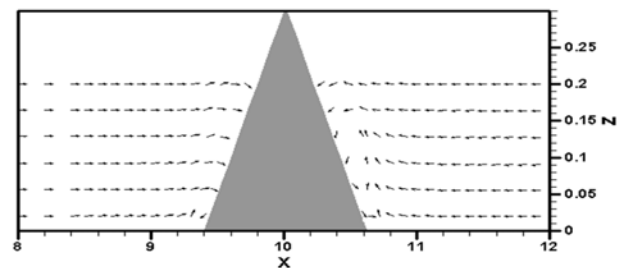


c. Bed cross-sectional slope = 10%

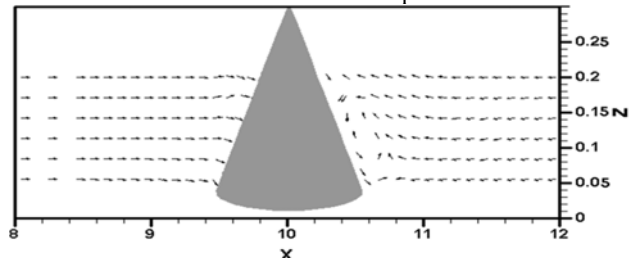
Fig.15 Velocity fields in the vertical plane at $y=0.25\text{m}$ for the groyne with structural slope= 1:0 at various cross-sectional bed slopes

5.5) Water elevation

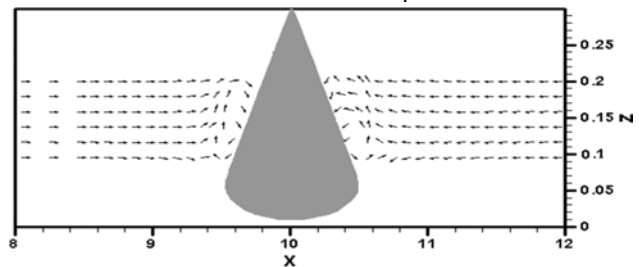
Finally, the numerical model results of the water elevations are described in this section. Fig. 17 illustrates the typical predicted water elevation profiles on $x-z$ planes around the groyne for various conditions. It can be seen from the figure that the water elevation increased at the upstream of the structure and decreased at the downstream of the groyne. Comparing of the model results for various bed slopes and model configurations have shown that by decreasing the structural slope and increasing the cross shore bed slope, the water elevations increased smoothly adjacent to the groynes.



a. Bed cross-sectional slope = 0%



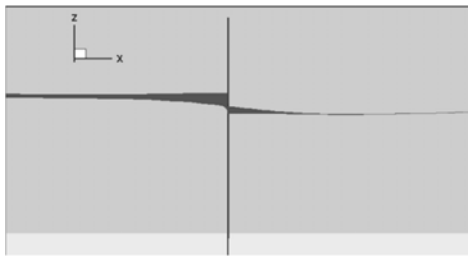
b. Bed cross-sectional slope = 5%



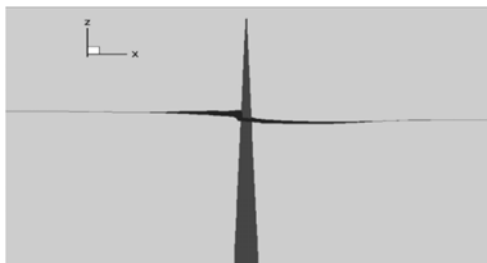
c. Bed cross-sectional slope = 10%

Fig.16 Velocity fields in the vertical plane at $y=0.25\text{m}$ for the groyne with structural slope = 1:2 at various cross-sectional bed slopes

It can be seen from the figure that for the vertical groyne on a flat bed there is not any vertical circulation cell. However, the vertical cells grew rapidly when the cross-sectional bed slope increased. Similar results have been achieved for the structural sloped groynes (see Fig. 16). Another comparison can be made for the two type groynes on a flat bed (i.e. Figs. 15(a) and 16(a)). Comparing of these model results shows that by increasing the sidewall of the groyne, the vertical components of the velocity decrease and this can reduce the scour depth at the toes of sidewalls.



a. Groyne with wall-groyne slope = 1:0 on the bed with cross-sectional slope = 5%



b. Groyne with wall-groyne slope = 1:1 on the flat bed

Fig.17 Variation of water surface in the X-Z plane

6 Conclusions

The main conclusions of this numerical model research can be summarized as follows:-

1. The model results shows that by increasing the cross-sectional bed slope the maxima magnitudes of velocities and their domains decreased. Also it has been found by decreasing the structural slope of groyne these values further decreased.
2. The model results have shown that by increasing the cross-sectional bed slope, the maxima values of the bed shear stresses reduced. Also, by decreasing the structural slope of the groyne, these values further decreased. This can be considered as one of the main conclusions of this study since the bed shear stress has an important role in scour process.
3. The model results have shown that by increasing the cross-sectional bed slope, the reattachment length increased, whereas the non-dimensional length of the reattachment decreased.
4. Comparing of the model results for the down-flows shows that by increasing the sidewall of the groyne, the vertical components of the velocity decrease and this can reduce the scour depth at the toes of the sidewalls.
5. Comparing of the all model results for various bed slopes and model configurations have shown that by decreasing the structural slope and increasing the bed slope, the water elevations increased smoothly adjacent to the groyne.

References

- [1] Shields F. D. Jr, Cooper C. M, Knight S. S (1995) Experiment in stream restoration. *J Hyd Eng* 121(6):494-502.
- [2] Fredsoe J, and Deigaard R (1992) *Mechanics of Coastal Sediment Transport*. Advanced Series on Ocean Engineering, Volume 3, World Scientific Publications.
- [3] Ouillon S, and Dartus D (1997) Three dimensional computation of flow around groyne. *J Hyd Eng* 123(11):962-970.
- [4] Uijtewaal W. S. J (2005) Effects of groyne layout on the flow in groyne fields: laboratory experiments. *J Hyd Eng* 131(9):782-791.
- [5] Molls T, Chaudhry M. H and Khan K.W (1995) Numerical simulation of 2-D flow near a spur-dike. *Advances in Water Resources* 18(4):227-236.
- [6] Tominaga A, Nagao M and Nezu I (1997) Flow structures and mixing processes around porous and submerged spur-dikes. *Environmental and Coastal Hydraulics*, 251-256.
- [7] Zhou Y, Michiue M and Hinokidani O (2000) A numerical study on the comparison of 3-D flow properties around submerged spur-dikes. *Annual J Hyd Eng, JSCE*, 44:605-610.
- [8] Uijtewaal W. S. J, Lehman D and Mazijk A (2001) Exchange processes between a river and its groyne fields: model experimental. *J Hyd Eng* 127(11):928-936.
- [9] Kuhnle R. A, Alonso C. A and Shieldsjr F. D (2002) Local scour associated with angled spur dike. *J Hyd Eng* 128(12):1087-1093.
- [10] Ettema R and Muste M (2004) Scale effects in flume experimental on flow around a spur dike in flatbed channel. *J Hyd Eng* 130(7): 635-646.
- [11] Yossef M. F. M (2004) The effects of the submergence level on the resistance of groynes: an experimental investigation. *The 6th Int. Conf. on Hydro-science and Engineering*, (ICHE)
- [12] Nagata N, Hosoda T, Nakato T and Muramoto Yoshio (2005) Three dimensional numerical around river hydraulic structures. *J Hyd Eng* 131(12):1074-1087.
- [13] Xuelin T, Xiang D and Zhicong C (2006) Large eddy simulation of three-dimensional flows around a spur dike. *Tsinghua Science & Technology* 11(1):117-123.
- [14] Chen C.J and Jaw S.Y (1998) *Fundamentals of Turbulence Modeling*. Taylor & Francis, USA.
- [15] Holtz K.P (1991) Numerical simulation of recirculating flow at groynes. *Computer Methods in Water Resources*, C.A Brebbia, D Quazar and D. Ben Sari, Eds, Springer Verlag, New York, Inc., New York, N.Y. 2(2): 463-477.
- [16] Fluent 5.2 (1998) *User's Guide*. Fluent Inc. Lebanon, New Hampshire, U.S.A.
- [17] Keshavarz, M.H, Hakimzadeh H and Ghaldarbandi R (2008) Three-dimensional numerical

simulation of flow pattern around perpendicular and inclined groynes with respect to various boundary conditions. J Marine Eng, Fall & Winter 2008-2009, 4(8):11-24.